CHAPTER 3

Mechanotransduction at the Cell Surface and Methods to Study Receptor Forces

RONG MA,[a] BRENDAN R. DEAL[a] AND KHALID SALAITA*[a,b]

[a] Department of Chemistry, Emory University, Atlanta, GA, USA; [b] Wallace H. Coulter Department of Biomedical Engineering, Georgia Institute of Technology and Emory University, Atlanta, GA, USA
*Email: k.salaita@emory.edu

3.1 Introduction

Mechanical forces play a critical role in modulating many cellular processes.[1] Once cells experience mechanical stimuli, including substrate rigidity, external forces, and endogenous forces, they dynamically transduce the mechanical input into biochemical signals. With these signals, cells adapt and respond to their microenvironments, as well as make decisions involving activation, migration, proliferation, differentiation, and apoptosis (Figure 3.1A).[2] These processes, known as mechanosensing and mechanotransduction, have been observed in various cells, including platelets, cancer cells, stem cells, and immune cells.[3] Receptors on the cell surface, including integrins, notch, T cell receptor (TCR), and B cell receptor (BCR), participate intensively in mechanically sensing the environment and guide the cell through decision-making processes.[4–7] This chapter will start with an introduction of cell receptor force transduction, specifically force interplay between integrins and T cell receptor and their ligands, as well as its role in the cellular response. Then we will introduce tools that have been

Biomaterials Science Series No. 12
Material-based Mechanobiology
Edited by Jun Nakanishi and Koichiro Uto

Published by the Royal Society of Chemistry, www.rsc.org

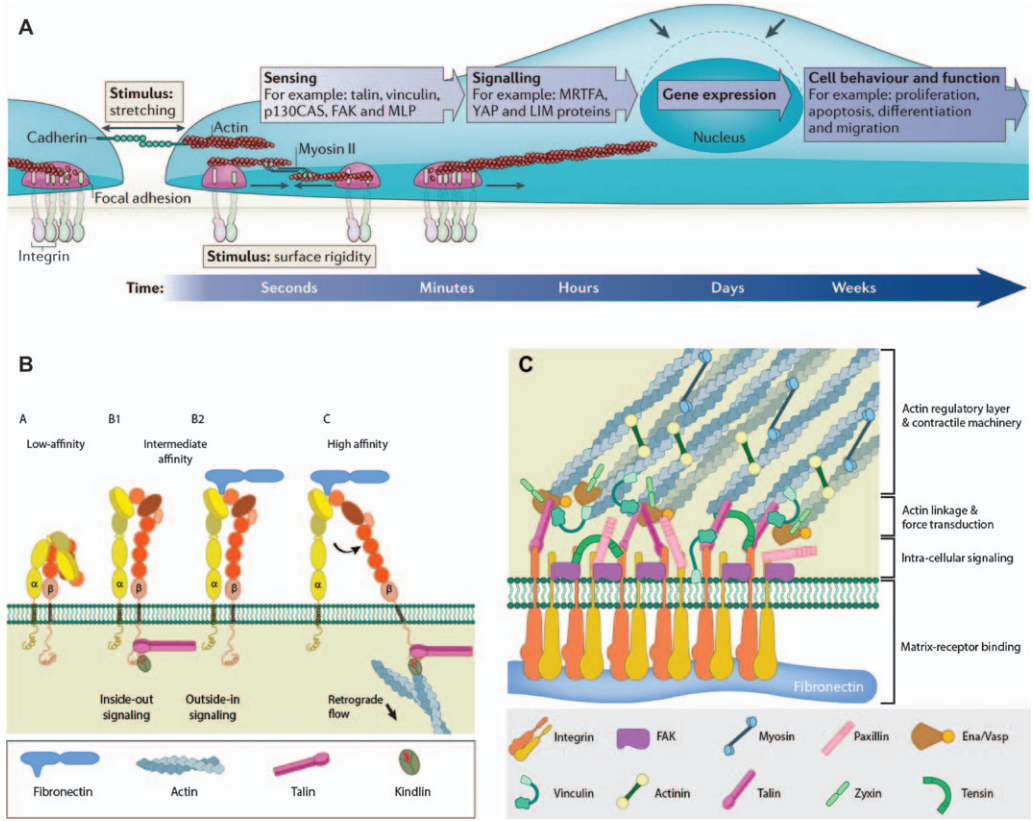

Figure 3.1 (A) Mechanotransduction modulates various cellular processes, integrin activation, and focal adhesion assembly. Reproduced from ref. 2 with permission from Springer Nature, Copyright 2014. (B) Integrin receptor in closed conformational A extending its extracellular domain to change into conformation B1. The cytoplasmic legs are further separated, resulting in another structural change from the extended closed conformation B1/2 to extended open conformation C, which has higher affinity binding to its ligand and facilitate mechanosensing and transduction. (C) Upon matrix-receptor binding, multiple proteins are recruited to assemble focal adhesions, which bridge the ECM with the cytoskeleton. Image provided courtesy of the Mechanobiology Institute, National University of Singapore [https://www.mechanobio.info/].

developed to study the receptor forces. Finally, this chapter will briefly discuss the future perspectives of using DNA-based tools to answer questions in the field of mechanobiology.

3.2 Mechanotransduction at the Cell Surface

3.2.1 Mechanotransduction Through Integrins

Integrins are adhesion proteins that bind to the extracellular matrix (ECM). An integrin molecule consists of an alpha and a beta subunit and forms a heterodimer. The integrin heterodimer has a large ectodomain, a transmembrane domain, and a short cytoplasmic tail. There are ~24 known integrin heterodimers mediating binding to diverse ECM molecules. One general ligand that these integrin ectodomains can recognize is a short amino acid sequence, arginine-glycine-aspartic acid (RGD motif), which is abundant in ECM proteins such as fibronectin and fibrinogen.[8] Studies suggest that integrins exist in different conformations that exhibit different ligand affinities. The integrins in the inactive bent form have lower affinity for their ligand, and the integrins in the active extended open form have high affinity (Figure 3.1B,C). The integrin constantly and rapidly changes between the different conformations to bind a ligand. Integrin signaling can be initiated by either proteins (talin and kindlin) binding on the cytoplasmic tail (“inside out”) or ECM ligands binding to its ectodomain (“outside in”), and these two pathways can drive integrin activation cooperatively.[9] When activated and bound to its ligand, integrin molecules are fully extended, with the cytoplasmic tails separated. The activated integrins can cluster and recruit multiple proteins inside the cells, including talin, vinculin, and paxillin, to form focal adhesions (FA).[10] FAs are coupled to the cytoskeleton and can transmit forces around tens of piconewtons (pN) to sense the environment.[11,12] As focal adhesions grow and mature, force transduction activates pathways such as Rho kinase-mediated phosphorylation of myosin II, which can then stabilize large focal adhesions. These stable focal adhesions aid in actin bundle assembly and stress fiber formation.[13–16] The actin stress fibers coupled to the FAs can transduce higher forces through actomyosin contractions and further facilitate mechanical signaling.[17,18] Consequently, through formation of FAs, integrins act as a main hub for mechanosensing and mechanotransduction in various cell types and facilitate activities like cell adhesion and migration.

3.2.2 Mechanotransduction Through T Cell Receptor

3.2.2.1 General Overview of T Cell Activation

T cells are critical in the adaptive immune system, as they constantly search for antigens and provide surveillance against viral infections and cancer. The T cell receptor (TCR) is a surface receptor that scans and tests the antigens by

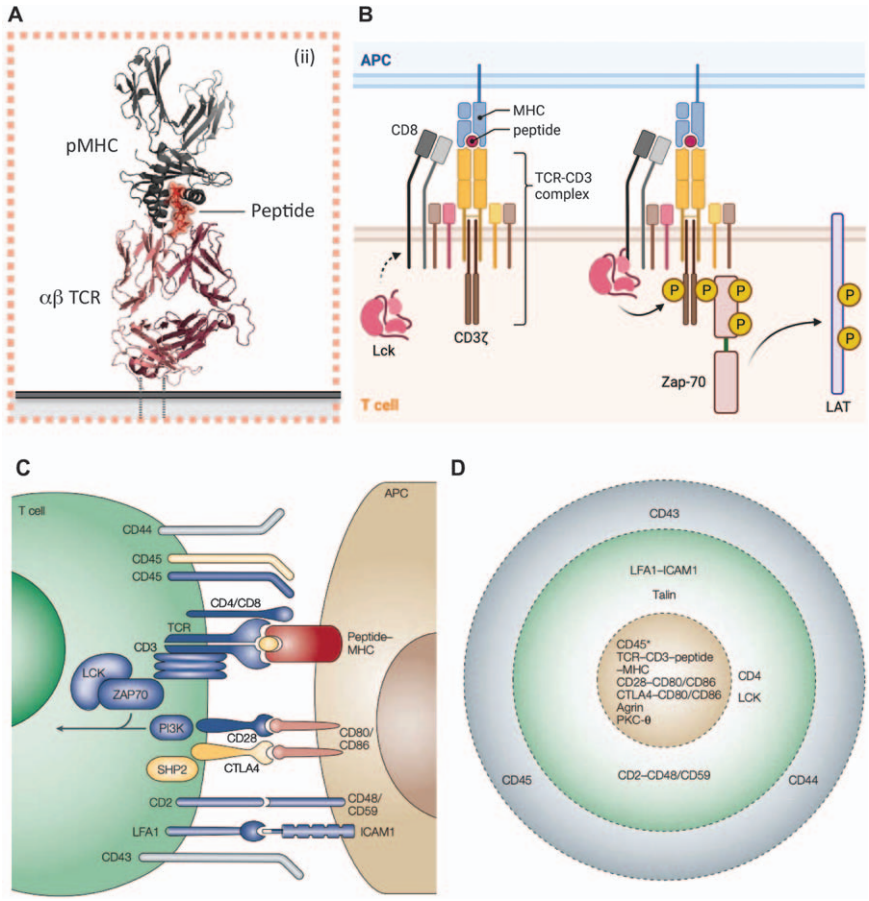

Figure 3.2 TCR–pMHC binding and its signaling pathway: (A) Structure of TCR binding to pMHC. Reproduced from ref. 19 with permission from Elsevier, Copyright 2018. (B) Signaling pathway after TCR triggering. (C) Side view showing the receptors and signaling proteins at the immune synapse formed between a T cell and an antigen presenting cell. (D) Top-down view showing the spatial organization of the proteins at the immune synapse. Reproduced from ref. 20 with permission from Springer Nature, Copyright 2003.

binding to them. TCR has high specificity for antigenic peptides that are presented by a major histocompatibility complex (pMHCs) on the surface of the antigen-presenting cell (Figure 3.2A), meaning it only recognizes antigenic peptides, exempting cells from autoimmune responses. TCR is a protein composed of a highly variable alpha chain and a beta chain, forming a heterodimer. TCR is usually expressed together with six invariant CD3 chain molecules that contain the signaling domains, forming a TCR–CD3 complex (Figure 3.2B). When it encounters a potent pMHC, TCR binds to the pMHC and initiates a discriminatory signaling cascade. The CD4 or CD8

coreceptors of TCR recruit Lck kinase, which can phosphorylate the signature tyrosine residues located at the signaling domain of the CD3 cytoplasmic tail, immunoreceptor tyrosine–based activation motifs (ITAMs). Phosphorylated ITAMs can bind to SH2 domain of the Zap70 kinase, and recruit Zap70 from the cytoplasm to the plasma membrane. Zap70 then phosphorylates linker for activation of T cells (LAT), which further recruits PLCγ1 and induces Ca^{2+} signaling. LAT also recruits adaptor proteins Grb2 and Gads, which bind to SOS and SLP-76 and lead to Ras, Rac, Rho GTPase activation.[19] This is an incredibly sensitive signaling cascade, which responds to an antigenic peptide within a few minutes after the first encounter with exceptional specificity.

Upon initial TCR triggering, the immune synapse (Figure 3.2C,D) is formed at the interface of the T cell and the antigen presenting cell (APC). The immune synapse is a highly organized dynamic structure, with a central region of the supramolecular activation complex (cSMAC), a peripheral region (pSMAC), and a distal ring (dSMAC). Together they form a ''bull's-eye'' pattern, with distinct spatiotemporal distribution of surface receptors and signaling molecules. The TCR–CD3 complex, as well as the CD28 coreceptor, is primarily located in the cSMAC upon activation. Adhesion ligands such as CD2 and LFA-1 (lymphocyte function-associated antigen 1) are relocated into the pSMAC, and the phosphatase CD45 is usually segregated to the dSMAC. Together, they facilitate T cells signaling and function, such as direct killing of the target cell.[20]

3.2.2.2 Proposed Mechanism for Initial TCR–pMHC Recognition

TCR binds to antigens while patrolling, and, upon antigen recognition, it can trigger a rapid whole cell response. This process can be initiated with as few as 1–2 cognate pMHC and within seconds to minutes. However, the affinity between TCRs and pMHCs in solution is usually between 1 μM and 10 μM, sometimes up to 100 μM, which does not provide much opportunity for antigen discrimination.[19–22] Therefore, a question that puzzles the field is how the TCR recognizes an antigen from the massive number of endogenous ligands that are displayed on antigen-presenting cell surfaces with explicit specificity and sensitivity.

Several models have been proposed to explain the remarkable ability of T cells to recognize specific antigens, including (1) kinetic segregation, (2) kinetic proofreading, (3) serial triggering, and (4) conformational change triggering model.[19,23] The kinetic segregation model proposed that the triggering is dependent on the segregation of large surface proteins like phosphatase CD45 from proteins that have small extracellular domains, such as TCR. The kinetic proofreading model suggests that the triggering is based on the differential binding durations, which provides the discrimination between strong and weak antigens. The serial engagement hypothesis suggested that successive rapid binding and unbinding events between clustered TCRs and a few pMHC is the mechanism of amplifying the

discrimination signal that drives TCR triggering. The conformational change model argues that the binding to pMHC induces a structural change in the TCR ectodomain, which exposed the signaling ITAMs inside the cells.

3.2.2.3 Mechanical Forces in TCR Triggering

Originally, these models were proposed without the involvement of mechanical forces. However, over the past decade, growing evidence suggests that molecular mechanical forces play an important role in T cell activation. Single-molecule force spectroscopy studies found that when a defined force is applied to immunoreceptors, the dissociation kinetics between the receptors and ligands is regulated by force (Figure 3.3). Moreover, the T cell triggering correlates with the duration of the receptor–ligand binding under a certain force (~10–20 pN). Specifically, the potent TCR–pMHC bindings exhibit a "catch-bond" behavior, *i.e.* the application of force prolongs the lifetime of the binding. Conversely, with weak agonist or antagonist peptides, the TCR exhibits a "slip-bond" behavior, *i.e.* the lifetime decreases upon force application (Figure 3.3E).[24] The catch-bond model can explain the differential potency of pMHCs when their affinities to TCR are similar.

These findings suggest that immunoreceptors are mechanosensors. Evident from the forces revealed by traction force microscopy, micropillars, and molecular tension probes, the T cells generate traction forces and transmit defined pN forces through TCR to pMHC, and the force is correlated with functional output like cytotoxic cell killing.[24,25] These complementary methods have provided new insight into the TCR triggering mechanism and further connected the role of cytoskeleton coordination in the T cell activation. Accordingly, the revised hypotheses of triggering mechanisms now including the role of force are discussed in the field and are shown in Figure 3.4.[23] Briefly, for the kinetic segregation model, the forces generated by cell cytoskeleton and transmitted through TCR can drive the segregation of CD45. And for the kinetic proofreading model, the catch-bond observation with single-molecule methods can explain the amplified discrimination between potent and weak antigens in terms of its 2D binding kinetics. For the serial engagement model, the engagement of the cytoskeleton would drive the clustering and potentially the successive bindings through the protrusive microvilli on the T cell surface.[26] For the conformational change model, a study using optical tweezers showed that the force can extend the FG loop on the TCR beta chain, prolong the lifetime, and initiate signaling,[27] though whether force induces conformational change on the cytoplasmic tail of TCR–CD3 complex is still unclear.

Taken together, mechanical force is a crucial parameter that regulates TCR triggering. However, as one of the most sensitive, specific, and efficient recognition-activation processes in biology, TCR triggering is more likely to be explained by a collective effort rather than by a single mechanism. For example, the initial fast bindings could extend the FG loop, prolong the lifetime, press on the CD3ε, and induce a TCR–CD3 conformational change,

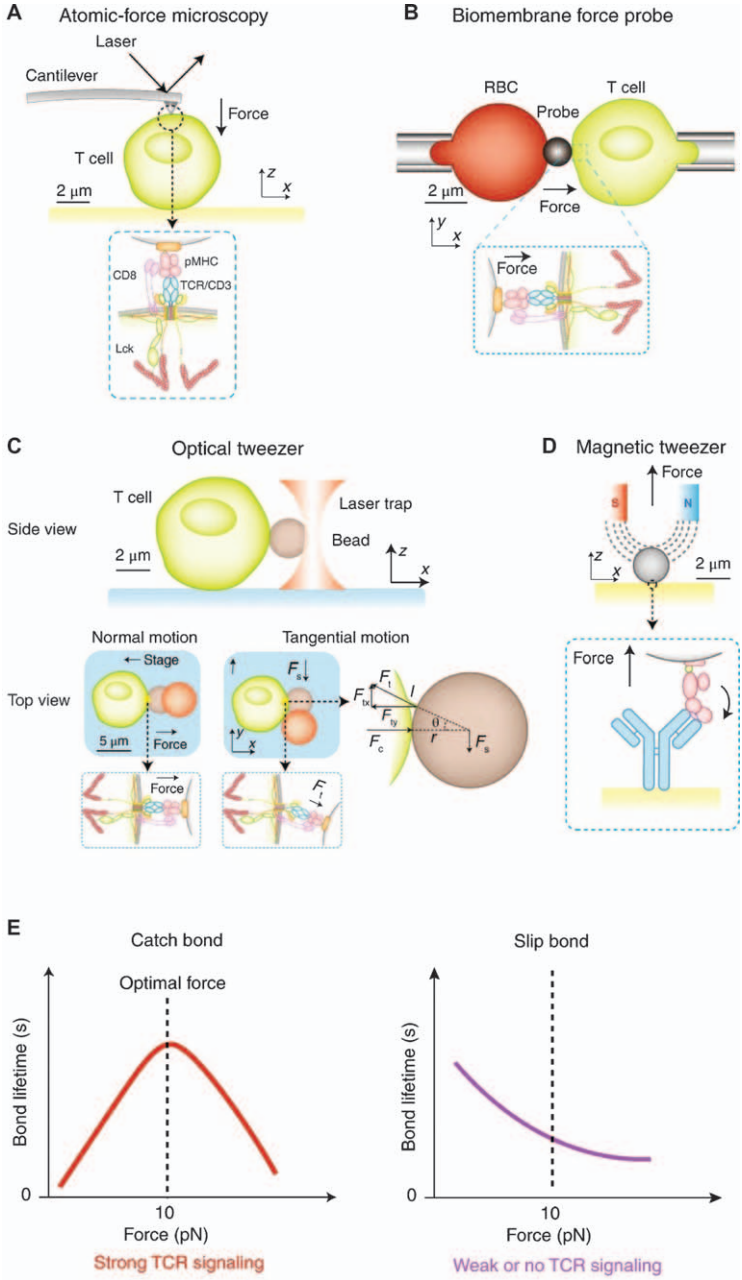

Figure 3.3 Single-molecule force spectroscopy methods to apply force to T cells: (A) Atomic force microscopy, (B) biomembrane force probe, (C) optical tweezer, and (D) magnetic tweezer are all used to apply an external force and interrogate the force contribution in TCR–pMHC binding. (E) Illustration of catch-bond and slip-bond. Reproduced from ref. 24 with permission from Springer Nature, Copyright 2019.

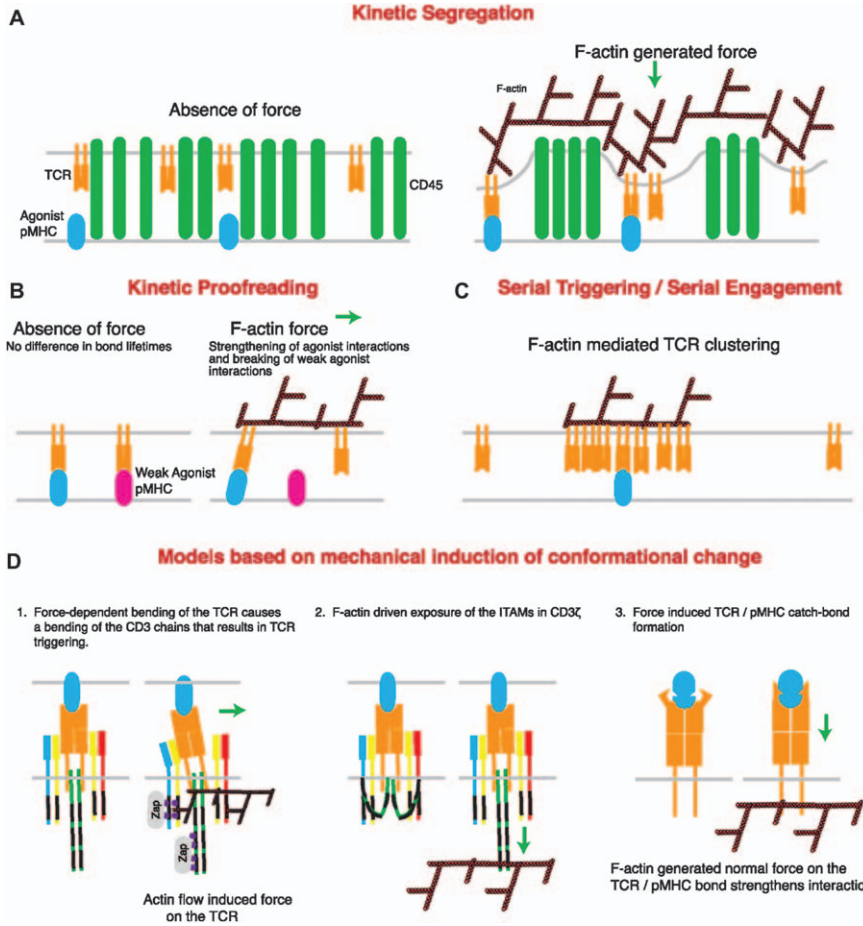

Figure 3.4 Revised models for TCR triggering with force and cytoskeleton engagement: (A) TCR force may contribute to the kinetic segregation of CD45. (B) Presence of force may contribute to the kinetic proofreading of the ligand by the TCR. (C) Cytoskeletal forces could drive TCR clustering and contribute to the serial engagement of TCR–antigen. (D) Forces transmitted through TCR could result in TCR conformational change, which may prolong the lifetime of TCR–antigen binding and facilitate phosphorylation. Reproduced from ref. 23, https://doi.org/10.3389/fimmu.2016.00068, under the terms of the CC BY 4.0 license https://creativecommons.org/licenses/by/4.0/.

which could further release the ITAMs and allow phosphorylation in the cytoplasmic tail. As the phosphorylation rapidly signals through Ca^{2+} to the cytoskeleton, the actin network could engage and mediate the rearrangement of the receptors, including the segregation of phosphatases and the clustering of TCRs, strengthen the mechanical test on the TCR–pMHCs, and contribute to a significantly amplified discrimination by exposing more phosphorylation sites.

3.3 Methods to Study Receptor Forces

Methods like traction force microscopy and micropillar arrays have been widely used in the field of mechanobiology to reveal these mechanical events during biological processes.[28,29] However, their relatively poor spatiotemporal resolution, as well as force sensitivity, has long been the bottleneck of uncovering more details of cell receptor mechanics (Figure 3.5).[30] The emergence of molecular tension probes in 2011 greatly enhanced the resolution of receptor force mapping. Our lab pioneered the use of entropic polyethylene glycol (PEG) as the force-sensing spring to report force in the range of 1–20 pN, but the ''analog'' force-responsive fluorescence signal (fluorescence intensity increases as force magnitude increases) could be confused with the percentage of opened probes in force mapping.[31,32] Conveniently, using nucleic acids for force sensing is advantageous, as it improves force mapping resolution and reports the ''digital'' force-responsive fluorescence signal (fluorescence switches on as duplex mechanically melts), simplifying data processing and interpretation.[33] Moreover, DNA offers unrivaled flexibility in multiple ways. First, the probe assembly is simple yet still allows for a tunable force threshold. Second, different chemical modifications can be incorporated easily for conjugation with a ligand, fluorophore, quencher, or surface. Third, the simple rules of Watson–Crick base pairing also allow the probes to be highly modular and programmable with other additional features.

3.3.1 DNA Mechanics

Because DNA is extensively used a mechanical probe, it is imperative to provide some background on the response of nucleic acids to external molecular forces. DNA is an elastic polymer, and its mechanical properties are often described

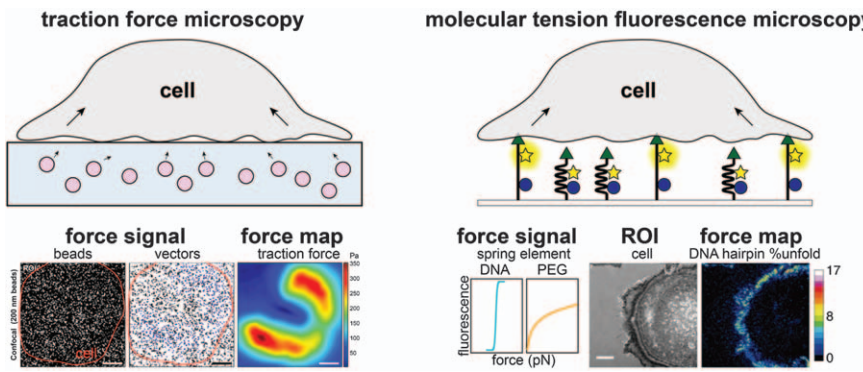

Figure 3.5 Force signal and force mapping with traction force microscopy (scale bar = 10 μm) *versus* molecular tension fluorescence microscopy (scale bar = 10 μm). Part of the figure, reproduced from ref. 29 with permission from American Chemical Society, Copyright 2020; part of the figure, reproduced from ref. 33 with permission from Springer Nature, Copyright 2014.

using the worm-like chain model (WLC) and specifically single-stranded DNA. The mechanical response of DNA under tensile force is usually characterized by single-molecule force spectroscopy methods, including optical tweezers, magnetic tweezers, and atomic force microscopy.[34,35] Various DNA structures have been examined under force, and among them, a few fundamental structural transitions have been intensively used for tool development in the field of DNA nanotechnology for mechanobiology studies.[36]

3.3.1.1 *DNA Hairpin Unfolding under Force*

For a simple DNA hairpin, its energy landscape can be simplified as two energy minima corresponding to the closed and open states that are separated by a single energy barrier. The application of stretching force ''tilts'' the energy landscape and shifts the free energy such that the closed state is destabilized, in contrast to the open state, which is stabilized. The external force that results in an equal probability of the open and closed states (free energy difference between the two states = zero) is described as the $F_{1/2}$ (Figure 3.6A). During the mechanical unfolding of the hairpin, the applied external force (work) must make up for the free energy of hybridization, as well as the free energy associated with stretching of the nucleotides.[35] Therefore, the $F_{1/2}$ can be defined as

$$F_{1/2} = (\Delta G_{\text{unfold}} + \Delta G_{\text{stretch}})/\Delta x \tag{3.1}$$

where ΔG_{unfold} is the free energy of hairpin unfolding at zero force, $\Delta G_{\text{stretch}}$ is the free energy of stretching the unfolded ssDNA at $F_{1/2}$, and Δx is the opening distance from folded to unfolded state. The $\Delta G_{\text{stretch}}$ can be calculated from a simple worm-like-chain (WLC) model,

$$\Delta G_{\text{stretch}} = \left(\frac{k_{\text{b}}T}{L_{\text{p}}}\right)\left[\frac{L_0}{4\left(\frac{1-x}{L_0}\right)}\right]\left[3\left(\frac{x}{L_0}\right)^2 - 2\left(\frac{x}{L_0}\right)^3\right], \tag{3.2}$$

where k_{b} is Boltzmann constant, L_{p} is the persistent length of DNA, T is temperature, L_0 is ssDNA contour length, and x is the hairpin extension. The Δx can be estimated from the contour length following 0.44 ± 0.02 nm per nt (with a 2.0 nm width of duplex DNA correction). The ΔG_{unfold} increases linearly with increasing stem GC% and stem length; however, increasing stem length also allows more energy to be stored, which affects $\Delta G_{\text{stretch}}$, and collectively defines the range of $F_{1/2}$ to within ~2–20 pN.[28]

3.3.1.2 *DNA Duplex Rupture under Force*

Unlike DNA hairpins, DNA duplex melting is irreversible. The same DNA duplex can have identical chemical and thermal stability but drastically

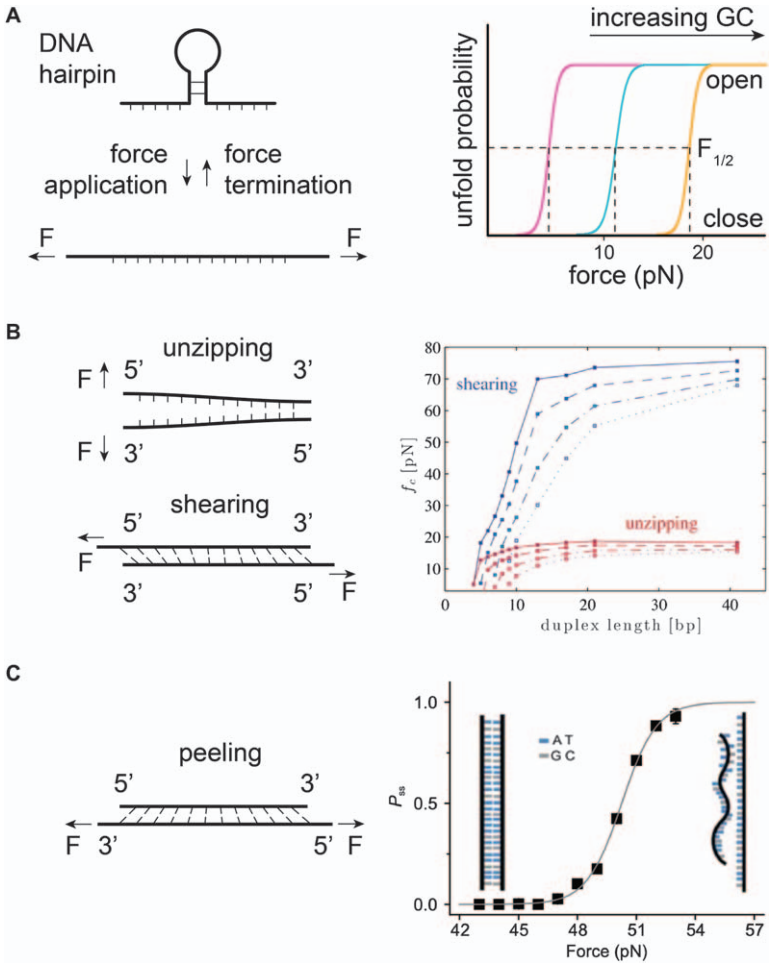

Figure 3.6 (A) Mechanical unfolding of DNA hairpin. (B) Mechanical rupture of DNA duplex. Part of the figure, reproduced from ref. 36 with permission from American Chemical Society, Copyright 2020. (C) Mechanical peeling of DNA duplex. Plot shows the transition and T_{tol} for a 28mer DNA duplex. Reproduced from ref. 41 with permission from Springer Nature, Copyright 2016.

different mechano-stability depending on the geometry of how force is applied (Figure 3.6B). When a short DNA duplex is stretched in an antiparallel manner (shearing, 5′–5′ or 3′–3′ pulling), the critical force at which 50% of the duplexes rupture (in a fixed time 2 s) increases with duplex length and plateaus at a certain length.[37] It can be described by the de Gennes model, which treats a DNA duplex as an elastic ladder and takes into account the hydrogen bond between base pairs. As the force is not evenly distributed on the base pairs, the base pairs that are bearing the load is a finite number, which results in a finite length x^{-1} that can be described with the spring

constant of the stretched DNA backbone Q and the spring constant of the stretched hydrogen bonds between base pairs R, where

$$x^{-1} = \sqrt{Q / 2R} \tag{3.3}$$

Therefore, in the de Gennes model, the rupture force for a DNA duplex in the shearing geometry can be described as

$$F = 2f_c \left[x^{-1} \tanh\left(x\frac{L}{2} \right) + 1 \right] \tag{3.4}$$

where f_c is the critical force for separating a single base pair (~3.9 pN), $x^{-1} = 6.8$ bp by magnetic tweezer characterizations, and L is the number of DNA base pairs.[7,37]

Another geometry of short DNA duplex rupture, unzipping mode (5′–3′ pulling perpendicularly to the duplex), can be treated as a single bp shearing, while the remaining base pairs are only thermally stabilizing the duplex. According to eqn (3.4), the rupture force is ~12 pN, which is very close to what has been measured experimentally.[38]

3.3.1.3 DNA Duplex Peeling under Force

DNA duplexes can also melt under force that is applied on the same strand (5′–3′ pulling), through a force-driven strand separation process known as peeling. Magnetic tweezers characterization showed that for short DNA duplexes under 5′–3′ pulling on the same strand, the melting is a two-state system with a transition state consisting of several base pairs (Figure 3.6C). The application of force contributes to the free energy needed for the DNA to transition from dsDNA to ssDNA. The critical force that induces this transition, T_{tol}, is defined as the critical force at which there is 50% ssDNA at a given time and is dependent on the GC%. For AT-rich short duplexes, the T_{tol} is usually below 65 pN, and peeling occurs before the DNA B-form to S-form transition.[39,40] Specifically, for a 24mer or a 28mer duplex in a magnetic tweezer study, the T_{tol} was found to be ~41 pN and ~50 pN for the 24mer and 28mer duplexes, respectively.[41]

3.3.2 DNA-based Molecular Force Sensing

Taking advantage of the mechanical melting properties of DNA molecules, DNA-based force probes have been invented to map and study the forces exerted from a receptor on the cell surface to its ligand. Typically, the force probes are comprised of a mechanical melting region, a fluorophore-quencher pair that reports mechanical melting events, and the ligand that the receptor of interest can recognize. These DNA-based molecular probes are often anchored on 2D surfaces to present the ligands to cells. After cells are plated onto these force probe-functionalized surfaces, the receptors

recognize, bind, and exert forces to the ligands. As the forces are transmitted through the DNA construct, if the force is greater than the $F_{1/2}$ or T_{tol} of the DNA construct, mechanical melting will occur, resulting in a change in the distance between the fluorophore and quencher, yielding a fluorescent signal to report this mechanical melting event. These probes can be reversible or irreversible depending on the structure of the DNA force-sensing region (Figure 3.7).

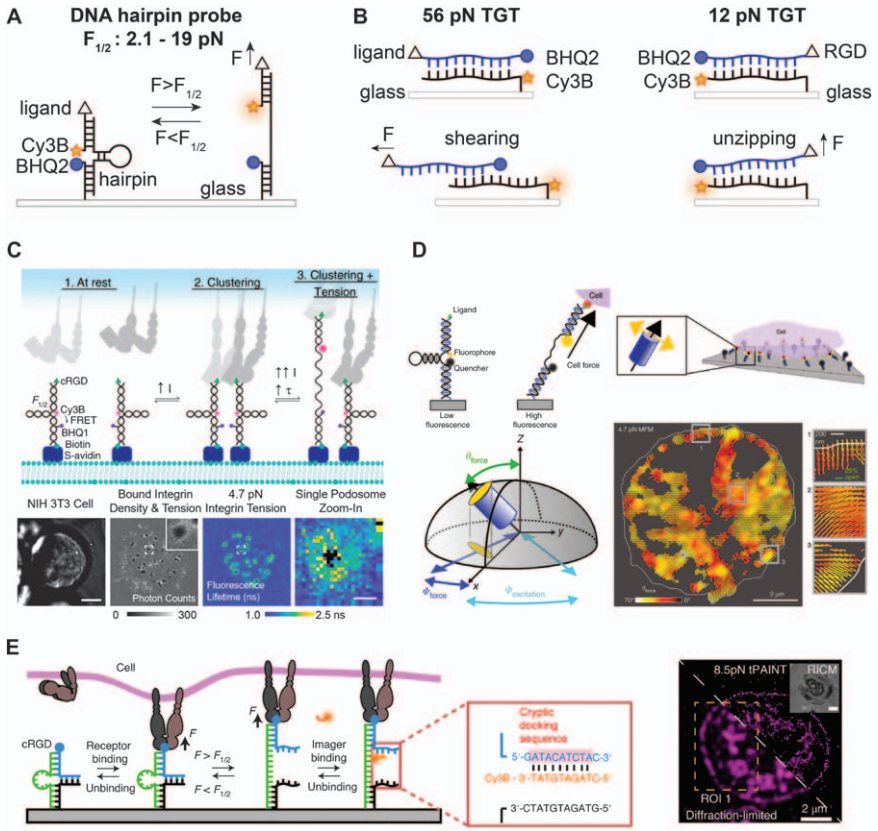

Figure 3.7 Classic reversible and irreversible DNA-based tension probes: (A) Reversible DNA-based hairpin tension probe with turn-on fluorescence upon hairpin unfolding. (B) Irreversible DNA-based tension gauge tether with turn-on fluorescence upon duplex rupture in different geometries. (C) Fluorescent lifetime imaging enables mapping of receptor clustering and force signal. Reproduced from ref. 49 with permission from Springer Nature, Copyright 2019. (D) Molecular force microscopy (MFM) with DNA hairpin probes reports the integrin force orientation. Reproduced from ref. 52 with permission from Springer Nature, Copyright 2018. (E) Live-cell super-resolved PAINT imaging of piconewton cellular traction forces. Reproduced from ref. 54 with permission from Springer Nature, Copyright 2020.

3.3.2.1 Reversible DNA Force Probes

DNA hairpin structures are incorporated as the force-sensing module due to their dynamic ability to unfold and refold with or without the presence of the force. DNA hairpin tension probes report the forces exceeding the threshold, $F_{1/2}$. As $F_{1/2}$ is dependent on the ΔG_{unfold} and $\Delta G_{stretch}$ as discussed in Section 3.3.1.1, one can easily tune the force threshold that the probes map by tuning the GC% and length of the hairpin stem. The first DNA hairpin tension probes were reported in 2014 by two groups independently. Chen and colleagues reported an all-covalent system by using a single-strand DNA with a stem-loop region, with modifications of a fluorophore, a quencher, and a peptide ligand RGD. With this molecular tension probe, they mapped the heterogeneous integrin forces in fibroblast focal adhesions.[42] Meanwhile, the Salaita lab pioneered a highly modular DNA hairpin tension probe system, comprised of three strands, a top strand with a ligand and a fluorophore, a bottom strand with a quencher and an anchoring moiety, and a hairpin strand that links them together. This multistrand design provided more flexibility for force mapping as opposed to the single-strand design, as one can easily change the force threshold of the probe by swapping the hairpin strand, which does not require any additional chemical modifications. One benefit of using a reversible force probe is that it provides low force threshold mapping. Our lab reported a small library of DNA hairpin tension probes ranging from 2.1 pN to 19 pN.[5,33] While providing great temporal resolution of the force dynamics, one disadvantage of the hairpin probes is that it only reports forces in real time. The force history information is difficult to capture because it refolds within microseconds once force is withdrawn. Another limitation is that the narrow force detection limit is not sufficient for receptors that can produce stronger forces. The latest generation of DNA tension probes now address these limitations and have expanded the capabilities of DNA tension probe technology.

3.3.2.2 Irreversible DNA Tension Probes

Irreversible DNA tension probes fail to provide temporal resolution of the force dynamics; however, they provide information on the receptor force history. Ha and coworkers first reported manipulation of the tension exerted through receptor–ligand binding with tension gauge tethers (TGT). The two geometries, unzipping and shearing, detect and tolerate peak tension of 12 pN and 56 pN, respectively.[7] Compared to hairpin probes, TGTs have a bigger range of force detection, which is tuned by positioning the ligand at different positions throughout the length of the duplex.[43] As a receptor mechanotransduction manipulating tool, the TGT is well suited, since the chemical cues it provides to cells are the same, while the mechanical cues are very different. However, as a force reporter, TGTs have two major drawbacks. First, the lowest T_{tol} for TGTs is 12 pN. Though there have been attempts to reach a lower force regime using a single-strand DNA wrapping

around the protein SSB, which achieved ~4 pN of T_{tol};[44] the other drawback remains: Once TGTs are ruptured, the mechanical signaling is terminated as well, inevitably affecting the function of the cell.

3.3.2.3 *Other Variations of the Probes to Answer Specific Mechanobiology Questions*

Building on the basic structure of DNA hairpins and TGTs, more DNA structures have been designed to investigate different biophysical questions at the cell–substrate interface. Wang and coworkers further developed the TGT library by positioning the ligand on different bases on the top strand, incorporating fluorophore-quencher pairs, and assembling multiplexing substrates, which further calibrated the integrin forces inside and outside FAs to a narrower rage.[43,45] To amplify the receptor force readout, a mechanically triggered isothermal polymerization reaction based on the TGT structure was reported, which has potential in evaluating mechanomodulatory drugs.[46] Additionally, DNA origami structures with multivalent hairpin force probes were reported, capitalizing on the ability of this self-assembly technique to present multiple ligands with precisely controlled spacing, proving to be a great tool to study the relationship between the force and clustering.[47] This method would also allow for investigating the cross-talk between different receptors during mechanotransduction.

To study forces on membranes, DNA force probes were also redesigned to be compatible with supported lipid bilayers (SLB). SLB is a fluid system, which means an increase in intensity cannot be directly attributed to mechanical pulling by the receptors. To solve this issue, two strategies have been reported to distinguish receptor clustering from receptor forces. In 2016, a ratiometric probe was published, which can report TCR clustering and TCR forces simultaneously on a fluid membrane.[48] In 2019, a fluorescent lifetime imaging method was published that was able to distinguish the receptor clustering and force signals (Figure 3.7C), in addition to investigating the force during podosome formation on a fluid membrane.[49] While FLIM can be a useful solution for mechanobiology studies in fluid systems, it also has a relatively poor temporal resolution (~60 s), which limited its application to less dynamic receptor forces. Apart from using SLBs to mimic the cell–cell interface, there are also attempts of mapping the force at the cell–cell junction. In 2017, a membrane DNA tension probe was tested at the cell–cell junction. Instead of being anchored on a 2D substrate, the DNA tension probe was anchored to the membrane of a cell through two cholesterol modifications *via* hydrophobic interaction.[50] It is, however, important to be aware of the stability of cholesterol probe anchoring, which could potentially cause false negative signals. Cholesterol can also become involved in cellular uptake, also potentially causing false signals.

To improve the receptor force signal produced by immune cells, which is generally difficult to detect, a mechanical information-storing DNA tension probe based on mechanically selective hybridization was developed.[51]

The ability of this probe to toggle between measuring real-time tension and accumulative tension made it versatile, allowing for applications in both static and migratory cells. The application in T cells revealed that they transmit >4.7 pN TCR forces to altered peptide ligands (APL) and that the mechanical sampling of APLs is correlated with their potency. In addition, it revealed that in activated T cells, PD1 transmits >4.7 pN forces to its ligand. This tension probe is among the most sensitive molecular force detection methods, ideal for visualizing weak and transient forces, as well as forces that are transmitted through low-density receptors; however, that the forces accumulated and amplified with this method are limited to 4.7–19 pN.

In addition to mapping the magnitude of the receptor forces and percentage opening of the probes, measuring the force orientation provides direct proof to support the hypotheses of whether the force orientation affects receptor mechanotransduction. To measure the receptor force orientation at the molecular level, molecular force microscopy (MFM) was invented by coupling fluorescence polarization microscopy with DNA hairpin probes.[52] Taking advantage of the stacking between the dye Cy3B and the DNA base pairs, MFM successfully reported the axial integrin force alignment during platelets activation, supporting a hypothesis of the involvement of lateral forces during platelets activation Figure 3.7D. However, one drawback of MFM is that the image acquisition is time-consuming (∼3.6 s), which makes it more suitable to measure the orientation of relatively less dynamic forces.

As more and more of the mysteries of receptor mechanics and its role in cell biology have been solved, recent research has been pushing imaging resolution to the nanometer level for force mapping. Wang and coworkers reported a cellular force nanoscopy (CFN) method in 2020, achieving 50 nm resolution in integrin force mapping.[53] This method utilizes a modified version of a conventional TGT, comprised of a DNase-resistant PNA/DNA duplex rather than a DNA/DNA duplex. The TGT is labeled with a fluorophore–quencher pair (Cy5–BHQ2); thus the Cy5 is dequenched once force is applied. This technique is straightforward and easy to implement with a TIRF microscope by following these steps: First, the dequenched Cy5 is bleached in 0.5–1 s; second, newly ruptured TGT molecules are imaged in the next frame; and third, the just imaged TGTs are bleached. By repeating this cycle, 50 nm resolution integrin force mapping is achieved in both migratory and stationary cells. One pitfall of this technique is that around 3% of the signal is false positive signal, coming from the dissociation of the TGTs during image acquisition. Another recent paper describes a relatively more complicated but powerful method to achieve super-resolved tension mapping. Leveraging DNA-points accumulation for imaging in nanoscale topography (DNA-PAINT) technique, the resolution is further improved to 25 nm.[54] The authors presented a real-time DNA tension probe featuring a strain-free force-sensing region with a cryptic docking site that is advantageous for a complementary imager strand to form a transient binding interaction (Figure 3.7E). By imaging the imager sampling of the

mechanically opened probes, a super-resolved tension map can be reconstructed. This method is also adaptable to the TGTs for mapping accumulative tension. Similar to CFN, one of the limitations of tPAINT is the temporal resolution. The other disadvantage is that tPAINT undersamples the mechanical events due to the imager on-rate. However, it is still superior given that it provides super-resolved tension mapping in both real time and the accumulative history.

3.4 Conclusion and Future Perspectives

In this chapter, we discussed receptor mechanics and the following signal transduction inside the cell using integrins and TCR as examples. The common methods of studying mechanobiology were briefly introduced, and the application of DNA as a force-sensing material was highlighted as a new direction in molecular mechanobiology. The force-sensing mechanisms of different basic DNA structures were discussed, followed by the introduction of powerful DNA-based tools to investigate the receptor mechanics from detecting the molecular receptor force to manipulating mechanical signaling.

Despite the encouraging advances that have been made, new techniques are needed to depict the receptor mechanics and its regulation. For example, mapping the cell mechanics inside and outside cells simultaneously can be powerful in elucidating how force is transmitted throughout different components within the cellular machinery. Coupling the DNA tension probes with protein-based FRET probes or measurement of actin retrograde flow is a good starting point for such investigations. Other interesting topics to explore further include the mechanical forces of virus particle entry, mechanics of engineered CAR-T cells, cell nuclear mechanosensing, differences in mechanics in healthy *versus* diseased cells, *etc.* To summarize, elucidating the relationship between tension and function needs extensive work, and there are many uncharted territories in the field of mechanobiology.

In addition to the mechanobiological questions, there are also some future directions for advancing DNA-based force detection. For example, nuclease-resistant DNA tension probes will allow force mapping for cells in culture, which will enable tracking of the mechanical footprint of stem cell differentiation. Moreover, integrating tension probes into 3D matrices or cell–cell junctions is critical, as it better mimics the biological environment than a 2D planar surface. The next generation of tools based on DNA nanotechnology that are used to study cell mechanics should also be tried to deconvolute the effects of force and work when evaluating the cell mechanics. Likewise, another domain that is forgotten is time. Specifically, interesting questions can be asked to further characterize the receptor mechanics in regard to the loading rate of the force, as well as the output power of a single receptor. Furthermore, tools that can detect molecular pushing or protrusive forces are equally important, as the cells not only mechanically sense the environment but also respond to it, especially at the cell–cell junction. We envision that a force-sensing/manipulating tool box

based on DNA nanotechnology will greatly aid the field of mechanobiology as it continues to assist research on cell mechanics from many different angles.

Acknowledgements

K.S. would like to acknowledge support from the National Institutes of Health (NIH) through R01GM124472 and 1R01GM131099, as well as the National Science Foundation (NSF) through CHE 2004126.

References

1. D. Mohammed, M. Versaevel, C. Bruyere, L. Alaimo, M. Luciano, E. Vercruysse, A. Proces and S. Gabriele, *Front. Bioeng. Biotechnol.*, 2019, **7**, 162.
2. T. Iskratsch, H. Wolfenson and M. P. Sheetz, *Nat. Rev. Mol. Cell Biol.*, 2014, **15**, 825.
3. Y. Chen, L. Ju, M. Rushdi, C. Ge and C. Zhu, *Mol. Biol. Cell*, 2017, **28**, 3134.
4. Y. Zhang, Y. Qiu, A. T. Blanchard, Y. Chang, J. M. Brockman, V. P.-Y. Ma, W. A. Lam and K. Salaita, *Proc. Natl. Acad. Sci. U. S. A.*, 2018, **115**, 325.
5. Y. Liu, L. Blanchfield, V. P.-Y. Ma, R. Andargachew, K. Galior, Z. Liu, B. Evavold and K. Salaita, *Proc. Natl. Acad. Sci. U. S. A.*, 2016, **113**, 5610.
6. K. M. Spillane and P. Tolar, *J. Cell Biol.*, 2017, **216**, 217.
7. X. Wang and T. Ha, *Science*, 2013, **340**, 991.
8. Z. Sun, M. Costell and R. Fassler, *Nat. Cell Biol.*, 2019, **21**, 25.
9. A. Banno and M. H. Ginsberg, *Biochem. Soc. Trans.*, 2008, **36**, 229.
10. D. A. Calderwood, I. D. Campbell and D. R. Critchley, *Nat. Rev. Mol. Cell Biol.*, 2013, **14**, 503.
11. L. B. Case and C. M. Waterman, *Nat. Cell Biol.*, 2015, **17**, 955.
12. F. Martino, A. R. Perestrelo, V. Vinarsky, S. Pagliari and G. Forte, *Front. Physiol.*, 2018, **9**, 824.
13. K. A. Beningo, K. Hamao, M. Dembo, Y. L. Wang and H. Hosoya, *Arch. Biochem. Biophys.*, 2006, **456**, 224.
14. C. Le Clainche and M. F. Carlier, *Physiol. Rev.*, 2008, **88**, 489.
15. J. Stricker, Y. Aratyn-Schaus, P. W. Oakes and M. L. Gardel, *Biophys. J.*, 2011, **100**, 2883.
16. P. W. Oakes, Y. Beckham, J. Stricker and M. L. Gardel, *J. Cell Biol.*, 2012, **196**, 363.
17. J. I. Lehtimaki, E. K. Rajakyla, S. Tojkander and P. Lappalainen, *eLife*, 2021, 10.
18. E. Kassianidou, C. A. Brand, U. S. Schwarz and S. Kumar, *Proc. Natl. Acad. Sci. U. S. A.*, 2017, **114**, 2622.
19. A. H. Courtney, W. L. Lo and A. Weiss, *Trends Biochem. Sci.*, 2018, **43**, 108.
20. J. B. Huppa and M. M. Davis, *Nat. Rev. Immunol.*, 2003, **3**, 973.

21. S. Valitutti, S. Muller, M. Cella, E. Padovan and A. Lanzavecchia, *Nature*, 1995, **375**, 148.
22. J. Hellmeier, R. Platzer, A. S. Eklund, T. Schlichthaerle, A. Karner, V. Motsch, M. C. Schneider, E. Kurz, V. Bamieh, M. Brameshuber, J. Preiner, R. Jungmann, H. Stockinger, G. J. Schutz, J. B. Huppa and E. Sevcsik, *Proc. Natl. Acad. Sci. U. S. A.*, 2021, **118**, e2016857118.
23. W. A. Comrie and J. K. Burkhardt, *Front. Immunol.*, 2016, **7**, 68.
24. C. Zhu, W. Chen, J. Lou, W. Rittase and K. Li, *Nat. Immunol.*, 2019, **20**, 1269.
25. R. Basu, B. M. Whitlock, J. Husson, A. Le Floc'h, W. Jin, A. Oyler-Yaniv, F. Dotiwala, G. Giannone, C. Hivroz, N. Biais, J. Lieberman, L. C. Kam and M. Huse, *Cell*, 2016, **165**, 100.
26. E. Cai, K. Marchuk, P. Beemiller, C. Beppler, M. G. Rubashkin, V. M. Weaver, A. Gerard, T.-L. Liu, B.-C. Chen and E. Betzig, *Science*, 2017, **356**, eaal3118.
27. Y. Feng, E. L. Reinherz and M. J. Lang, *Trends Immunol.*, 2018, **39**, 596.
28. V. P. Y. Ma and K. Salaita, *Small*, 2019, **15**, 1900961.
29. A. Stubb, R. F. Laine, M. Miihkinen, H. Hamidi, C. Guzman, R. Henriques, G. Jacquemet and J. Ivaska, *Nano Lett.*, 2020, **20**, 2230.
30. W. J. Polacheck and C. S. Chen, *Nat. Methods*, 2016, **13**, 415.
31. D. R. Stabley, C. Jurchenko, S. S. Marshall and K. S. Salaita, *Nat. Methods*, 2011, **9**, 64.
32. Y. Liu, K. Yehl, Y. Narui and K. Salaita, *J. Am. Chem. Soc.*, 2013, **135**, 5320.
33. Y. Zhang, C. Ge, C. Zhu and K. Salaita, *Nat. Commun.*, 2014, **5**, 5167.
34. S. Cocco, J. Yan, J. F. Leger, D. Chatenay and J. F. Marko, *Phys. Rev. E*, 2004, **70**, 011910.
35. M. T. Woodside, W. M. Behnke-Parks, K. Larizadeh, K. Travers, D. Herschlag and S. M. Block, *Proc. Natl. Acad. Sci. U. S. A.*, 2006, **103**, 6190.
36. M. Mosayebi, A. A. Louis, J. P. Doye and T. E. Ouldridge, *ACS Nano*, 2015, **9**, 11993.
37. K. Hatch, C. Danilowicz, V. Coljee and M. Prentiss, *Phys. Rev. E*, 2008, **78**, 011920.
38. S. Cocco, R. Monasson and J. F. Marko, *Proc. Natl. Acad. Sci. U. S. A.*, 2001, **98**, 8608.
39. X. Zhang, H. Chen, H. Fu, P. S. Doyle and J. Yan, *Proc. Natl. Acad. Sci. U. S. A.*, 2012, **109**, 8103.
40. X. Zhang, Y. Qu, H. Chen, I. Rouzina, S. Zhang, P. S. Doyle and J. Yan, *J. Am. Chem. Soc.*, 2014, **136**, 16073.
41. Z. J. Yang, G. H. Yuan, W. L. Zhai, J. Yan and H. Chen, *Sci. China Phys. Mech.*, 2016, **59**, 680013.
42. B. L. Blakely, C. E. Dumelin, B. Trappmann, L. M. McGregor, C. K. Choi, P. C. Anthony, V. K. Duesterberg, B. M. Baker, S. M. Block, D. R. Liu and C. S. Chen, *Nat. Methods*, 2014, **11**, 1229.
43. Y. Wang, D. N. LeVine, M. Gannon, Y. Zhao, A. Sarkar, B. Hoch and X. Wang, *Biosens. Bioelectron.*, 2018, **100**, 192.

44. F. Chowdhury, I. T. Li, T. T. Ngo, B. J. Leslie, B. C. Kim, J. E. Sokoloski, E. Weiland, X. Wang, Y. R. Chemla, T. M. Lohman and T. Ha, *Nano Lett.*, 2016, **16**, 3892.
45. Y. Wang and X. Wang, *Sci. Rep.*, 2016, **6**, 36959.
46. V. P. Ma, Y. Liu, K. Yehl, K. Galior, Y. Zhang and K. Salaita, *Angew. Chem., Int. Ed.*, 2016, **55**, 5488.
47. P. K. Dutta, Y. Zhang, A. T. Blanchard, C. Ge, M. Rushdi, K. Weiss, C. Zhu, Y. Ke and K. Salaita, *Nano Lett.*, 2018, **18**, 4803.
48. V. P. Ma, Y. Liu, L. Blanchfield, H. Su, B. D. Evavold and K. Salaita, *Nano Lett.*, 2016, **16**, 4552.
49. R. Glazier, J. M. Brockman, E. Bartle, A. L. Mattheyses, O. Destaing and K. Salaita, *Nat. Commun.*, 2019, **10**, 4507.
50. B. Zhao, C. O'Brien, A. Mudiyanselage, N. Li, Y. Bagheri, R. Wu, Y. Sun and M. You, *J. Am. Chem. Soc.*, 2017, **139**, 18182.
51. R. Ma, A. V. Kellner, V. P.-Y. Ma, H. Su, B. R. Deal, J. M. Brockman and K. Salaita, *Proc. Natl. Acad. Sci. U. S. A.*, 2019, **116**, 16949.
52. J. M. Brockman, A. T. Blanchard, V. M. Pui-Yan, W. D. Derricotte, Y. Zhang, M. E. Fay, W. A. Lam, F. A. Evangelista, A. L. Mattheyses and K. Salaita, *Nat. Methods*, 2018, **15**, 115.
53. Y. Zhao, K. Pal, Y. Tu and X. Wang, *J. Am. Chem. Soc.*, 2020, **142**, 6930.
54. J. M. Brockman, H. Su, A. T. Blanchard, Y. Duan, T. Meyer, M. E. Quach, R. Glazier, A. Bazrafshan, R. L. Bender, A. V. Kellner, H. Ogasawara, R. Ma, F. Schueder, B. G. Petrich, R. Jungmann, R. Li, A. L. Mattheyses, Y. Ke and K. Salaita, *Nat. Methods*, 2020, **17**, 1018.